Temperature-dependent energy levels of electrons on liquid helium

E. Collin,* W. Bailey, P. Fozooni, P. G. Frayne, P. Glasson, K. Harrabi,† and M. J. Lea‡
Department of Physics, Royal Holloway, University of London, Egham, Surrey TW20 0EX, United Kingdom
(Received 2 August 2017; revised manuscript received 13 November 2017; published 20 December 2017)

We present measurements of the resonant microwave absorption between the Rydberg energy levels of surface-state electrons on the surface of superfluid liquid helium, in the frequency range 165–220 GHz. The resonant frequency was temperature dependent. The experiments are in agreement with recent theoretical calculations of the renormalization of the electron energy levels due to zero-point and thermal ripplons. The temperature-dependent contribution to the linewidth $\gamma(T)$ for excitation to the first excited state at 189.6 GHz is compared with other measurements and theoretical predictions.

DOI: 10.1103/PhysRevB.96.235427

I. INTRODUCTION

Electrons above the surface of liquid helium [1] are a fundamental two-dimensional conducting system. The electrons move in a potential well formed by a high potential barrier at the liquid surface and the attractive Coulomb potential of a weak positive image charge in the helium, $U(z) = -Ze^2/4\pi\varepsilon_0 z$, with $Z = (\varepsilon - 1)/4(\varepsilon + 1) = 0.007$. This gives a hydrogenlike spectrum, with energy levels $E_m \approx -R_e/m^2$, where the effective Rydberg energy $R_e = m_e e^4 Z^2/8h^2\varepsilon_0^2 \approx 0.67$ meV for liquid ^{4}He, $m(\geqslant 1)$ is the quantum number, and ε is the dielectric constant of the helium.

For 2D free electrons, the Rydberg levels give a series of subbands. Microwave transitions between the subbands were first observed by Grimes *et al.* [2] above 1.2 K for transitions from the ground state to the excited states, $m = 2,3$. Because of the asymmetry of the wave functions, these energy levels can be tuned with a vertical electric field E_z in a linear Stark effect. The resonant frequency $f_{21} = (E_2 - E_1)/h$ increases from 125.9 GHz in zero holding field up to 220 GHz for $E_z = 17.5$ kV/m. Lambert and Richards [3] extended the frequency range up to 765 GHz using a far-infrared laser.

Édel'man [4] and later Volodin and Édel'man [5] indirectly probed the Rydberg states, on both liquid ^{4}He and ^{3}He, by measuring the photoconductivity when the electrons were excited by incident microwaves.

Collin *et al.* [6] extended the measurements on liquid ^{4}He down to the ripplon scattering region below 0.7 K**.** They also investigated the absorption of microwaves at high powers and low temperatures in the nonlinear region, but underestimated the effects of electron heating. We now present an extended analysis of these experiments and, in particular, unpublished results on the temperature dependence of the resonance frequency $f_{21}(T)$ in comparison with recent theory.

Isshiki *et al.* [7] measured the microwave absorption for electrons on liquid ^{3}He from 0.01 to 1 K, with some experiments on liquid ^{4}He. Further microwave experiments have explored nonlinear effects in electrons on helium [8–12].

The theory was given by Ando [13] for both the gas-atom and ripplon scattering regimes. This underestimates the linewidth $\gamma(T)$ for vapor-atom scattering by a factor of 1.6 on ^{4}He and 2.1 on ^{3}He.

The binding energy of a surface-state electron to liquid helium is a conceptually simple problem, yet remains controversial. Grimes *et al.* [2] modeled this using an instructive empirical potential

$$U(z) = \frac{-Ze^2}{4\pi\varepsilon_0(z+b)} \quad \text{for } z > 0$$
$$= V_0 \quad \text{for } z \leqslant 0. \tag{1}$$

The effect of V_0 is to lower the ground-state energy, as the electron wave function penetrates into the helium with a decay length $\delta = 0.195$ nm for $V_0 = 1.0$ eV, and hence to increase the transition frequency f_{21}. A diffuse helium surface increases the ground-state energy. The fractional correction to f_{21} is $14(\delta - b)/3a_B$, where a_B is the effective Bohr radius (7.6 nm for electrons on ^{4}He). Grimes *et al.* [2] fitted the data to $V_0 = 1.0$ eV and $b = 0.104$ nm while Volodin and Édel'man [5] found $V_0 = 1.3\,s$eV and $b = 0.125$ nm for ^{3}He.

There have been many phenomenological models [2,5,14–17] for the electron energy spectrum. Most recently, Degani *et al.* [18] estimated the temperature dependence, predicting a large, almost linear decrease with temperature for $E_z = 0$.

But, these models treat the surface profile and hence the potential seen by the electrons, as static, although it can be temperature dependent. Zero-point and thermal ripplons on the helium surface [19] contribute to the diffuse surface or interfacial profile [20,21]. The electrons also react adiabatically to ripplons. Dykman *et al.* [22] show this renormalizes the electron energy spectrum at zero temperature and gives a nonlinear temperature dependence of the resonant frequencies down to the lowest temperatures. This ripplon-induced frequency shift, arising from the combination of a high interface barrier and a randomly distorted surface, including both zero-point and thermal ripplons, is subtle and involves both one-ripplon and two-ripplon interactions. This effect is a condensed-matter analog of the Lamb shift in the H atom, in which the electron wave function is "blurred" by interactions with zero-point photons in free space, giving a small shift in the binding energy.

*Present address: Institut Néel, CNRS & Université Grenoble Alpes, 25 rue des Martyrs, BP166, F-38042, Grenoble Cedex 9, France.
†Present address: Physics Department and Center of Research Excellence in Renewable Energy, King Fahd University of Petroleum and Minerals, 31261 Dhahran, Saudi Arabia.
‡Corresponding author: m.lea@rhul.ac.uk

The theory contains diverging terms from short-wavelength ripplons but these effectively cancel, leaving only a small increase in the energy levels with temperature $\Delta E_m(T)$. The corresponding temperature-dependent shift of the resonant frequency f_{21} is

$$\Delta f_{21}(T) = [\Delta E_2(T) - \Delta E_1(T)]/h < 0. \quad (2)$$

This paper describes measurements of the resonant microwave absorption of surface-state electrons on liquid ^{4}He to temperatures below 1 K. Measurements of the linewidth $\gamma_{21}(T)$ are presented and compared with other experiments and the theory of Ando [13]. The temperature dependence of the resonant frequency $\Delta f_{21}(T)$ is in good agreement with Dykman *et al.* [22] below 1 K.

II. MICROWAVE ABSORPTION

A. Lorentzian line shape

The microwave coupling between the electronic wave functions on helium is very strong with a dipole transition length z_{21} between the ground state $\psi_1(z)$ and the first excited state $\psi_2(z)$

$$z_{21} = \int \psi_1^*(z) z \psi_2(z) \mathrm{d}z, \quad (3)$$

which increases from $z_{21} = 0.59 a_B = 4.25$ nm for $E_z = 0$ to $z_{21} = 5.14$ nm for $E_z = 10.6$ kV/m, corresponding to $f_{21} = 190$ GHz. In the low-power limit, the integrated microwave absorption, normalized to the peak, is expected to have a Lorentzian line shape [13]

$$L(\delta f, \gamma) = \frac{\gamma^2}{\delta f^2 + \gamma^2}, \quad (4)$$

where $\delta f = f - f_{21}$. The microwave linewidth γ for electrons on helium has been calculated by Ando [13]. Two contributions can be distinguished, $\gamma = \gamma_1 + \gamma_2$. The first contribution γ_1 comes from the intersubband transitions from the excited state to the ground state with a transition rate $1/\tau$, with $\gamma_1 = 1/2\tau$ for gas-atom scattering, with

$$\frac{1}{\tau} = \frac{\sigma_a N_g(T)}{4 m_e a_B} \int_0^\infty \psi_1^2(z) \psi_2^2(z) \mathrm{d}z. \quad (5)$$

The second term corresponds to decoherence, from intrasubband scattering with no transition in the Rydberg state, with $\gamma_2 = 1/\tau_2$. The scattering time τ_2 for gas-atom scattering (equivalent to δ-function scattering) is given by

$$\frac{1}{\tau_2} = \frac{\sigma_a N_g(T)}{4 m_e a_B} \int_0^\infty \left[\psi_1^2(z) - \psi_2^2(z)\right]^2 \mathrm{d}z, \quad (6)$$

where $\sigma_a = 4.98 \times 10^{-20}$ m^2 is the helium atom scattering cross section and the vapor atom number density $N_g(T) = (2\pi m_4 kT/h^2)^{3/2} \exp(-7.17/T)$, where m_4 is the mass of a ^{4}He atom. The total temperature-dependent linewidth is given by

$$\gamma(T) = AT + BN_g(T), \quad (7)$$

where the first term is due to ripplon scattering. Coefficients A and B depend weakly on the holding field E_z [13].

Experimental linewidths $\gamma(T)$ in this paper are half-widths at half-height, given in frequency units of MHz, as converted from the measured voltage sweeps in V_z with a gradient $\beta = 2.44$ GHz/volt [6].

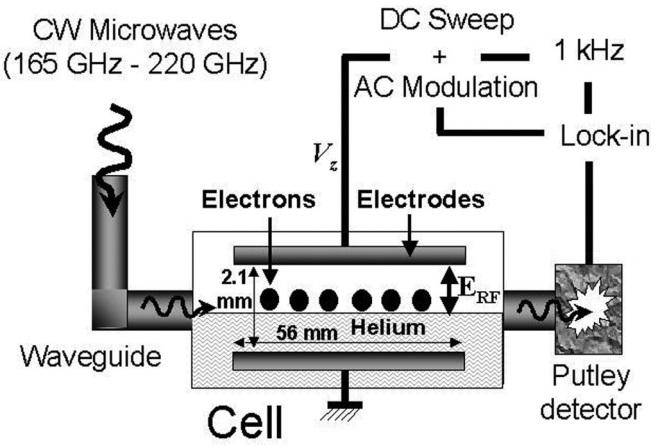

FIG. 1. Schematic diagram of the microwave cell [23]. The cell was half-filled with liquid helium as a substrate for the surface-state electrons. Vertically polarized microwaves were transmitted through the cell and detected by an InSb Putley detector. The vertical electric field E_z was swept through the microwave resonance. The field was ac-modulated and the modulated microwave signal was detected using a lock-in amplifier.

B. Microwave cell

Microwave experiments were performed at frequencies between 165 and 260 GHz, although most were done at 189.6 GHz. Further information about the microwave system is given in Supplemental Material [23].

The microwave cell is shown schematically in Fig. 1. The electrons were held above the liquid helium between capacitor plates $D = 2.075$ mm apart, which formed a flat cylindrical cavity, 56 mm in diameter. The upper and lower electrodes consisted of a central circular disk, surrounded by an annular ring. The lower ring was divided into four segments. The electrons were produced by thermionic emission from a pulsed filament in the upper cell.

The vertical separation of the cell was determined by two factors. First, the capillary length of liquid helium, $l_c = (\eta/\rho g)^{0.5} = 0.50$ mm, where η is the surface tension and ρ is the density of the liquid helium. When the cell is almost full, capillary rise will produce a "bubble" in the center of the cell of thickness $2l_c$ (like a spirit level) and the cell would then fill from the circumference. Hence it is not possible to have a stable and flat helium surface across the center of the cell with $D < 4l_c = 2.0$ mm, and this is the minimum height of the cell. The second reason is that the propagating microwave mode required is $p = 2$, where p is the number of standing half-wavelengths along the z axis [23]. For this mode the z-axis component of the microwave field is a maximum on the surfaces of the upper and lower electrodes and in the middle of the cell, at the helium surface where the electrons are distributed. The low-frequency cutoff for the $p = 2$ mode is $f_c \approx c/D = 150$ GHz, well below the operating frequency. Microwave transmission experiments clearly showed the onset of these modes in test cavities, as

the frequency was increased above cutoff. The central part of the cell forms a microwave pillbox cavity, with a complicated series of TM mode resonances as the microwave frequency was swept. The in-plane wavelength at 190 GHz is about 2.3 mm and the radial intensity distribution will form a pattern of nodes and antinodes from radial and azimuthal standing waves.

Continuous-wave microwaves were used with two ac electric field modulation schemes. Sine-wave modulation of V_z, typically 10 mV rms at 0.5 to 10 kHz, was used to measure the differential absorption $\alpha' = \mathrm{d}\alpha/\mathrm{d}V_z$ with a lock-in amplifier and integrated to obtain the absorption line shape $\alpha(V_z)$. Alternatively, large-amplitude square-wave modulation, typically ± 1.5 V, much bigger than the linewidth, gave the microwave absorption line directly, without numerical integration. Both schemes gave identical results at low-power levels. The modulation was imposed by applying equal in-phase and antiphase voltages to the upper and lower electrodes.

C. Electric holding field

For each experiment, fixed-frequency microwaves were used. The frequency $f_{21}(T)$ was tuned through resonance using the vertical holding field $E_z = E_{z1} + E_{z2}$, which is proportional to the voltage difference $\Delta V = V_{\mathrm{upper}} - V_{\mathrm{lower}}$ the capacitor plates

$$E_{z1} = \frac{-\Delta V}{(D - d + d/\varepsilon)}, \tag{8a}$$

where D is the vertical separation of the cell electrodes and d is the helium depth. The field was swept by symmetrically sweeping the potentials on the upper and lower electrodes, to maintain a constant potential on the electron sheet. To confine and hold surface electrons, $\Delta V = V_{\mathrm{upper}} - V_{\mathrm{lower}} < 0$. However in the experimental plots and discussion we define $V_z = V_{\mathrm{lower}} - V_{\mathrm{upper}} > 0$ as the pressing voltage, giving an upward pressing field E_z for the negatively charged electrons.

The field also depends on the electron density n. The density term E_{z2} is more subtle. For a uniform two-dimensional electron sheet in a grounded parallel-plate capacitor partly filled with dielectric, the induced charges produce a vertical field above the dielectric

$$E_{z2} = -\frac{ne}{2\varepsilon_0}\frac{(D - d - d/\varepsilon)}{(D - d + d/\varepsilon)}. \tag{8b}$$

But, this expression assumes that the polarization charges $ne(\varepsilon - 1)/(\varepsilon + 1)$ in the upper surface of the liquid helium are uniformly distributed. For electrons which are much closer to the helium surface than their in-plane spacing ($z \ll n^{-1/2}$), individual image charges give rise to the $1/z$ binding potential for each electron and should not be included in E_z. Hence, the constant electric field seen by individual electrons close to the helium surface is then given by

$$E_z = \frac{-\Delta V}{(D - d + d/\varepsilon)} + \frac{ne}{\varepsilon_0(\varepsilon + 1)}\frac{(D - 2d)}{(D - d + d/\varepsilon)}. \tag{8c}$$

The field E_z is independent of n only if the helium surface is at the geometrical center of the cell, $d = D/2$. For $z \gg n^{-1/2}$ the density-dependent field is given by Eq. (8b).

D. Electrons on liquid helium

The cell was filled with ultra-pure ^{4}He, with a ^{3}He/^{4}He concentration ratio $<10^{-13}$ [24]. The helium level in the cell was monitored during filling by measuring the capacitance between the upper and lower electrodes. The cell was leveled by charging the helium with electrons from a pulsed filament, and then driving the upper central electrode with a 10-kHz ac voltage and measuring the ac current to the four segmented electrodes on the lower electrode. The cryostat was tilted using air mounts to balance these four currents, thus leveling the helium in the cell. The tilt of the cryostat was continuously monitored during the experiments using variable resistance displacement devices on the cryostat top plate.

The electron density n was measured by using a Corbino electrode geometry to measure the magnetoconductivity [25]. A 10-kHz ac modulation was applied to the central electrode and the ac current flowing to the outer ring via the electrons was measured. A resistive phase shift $\varphi \propto 1/\sigma_{xx}$ is observed and hence σ_{xx} can be determined. In zero magnetic field $\sigma_0 = ne\mu$, where μ is the electron mobility. In a small perpendicular magnetic field B (<1 T), the Drude law holds [25], with $\sigma_0/\sigma_{xx}(B) = 1 + \mu^2 B^2$. Magnetoconductivity measurements enabled both $\sigma_0 = ne\mu$ and μB to be found independently, allowing μ and n to be determined. The values of μ were in good agreement with previous experiments [25]. The electron density profile was uniform out to a radius of about 27 mm.

III. RESULTS AND ANALYSIS

A. Resonant frequency

As the vertical holding field E_z was swept over a wide range at a fixed microwave frequency, a series of absorption peaks was observed as shown in Fig. 2 at a frequency of 220 GHz. These correspond to transitions from the ground state (subband), $m = 1$, to higher Rydberg states (subbands) $m = M$, as the Coulomb potential well changes with E_z. In these experiments we are primarily interested in the transition

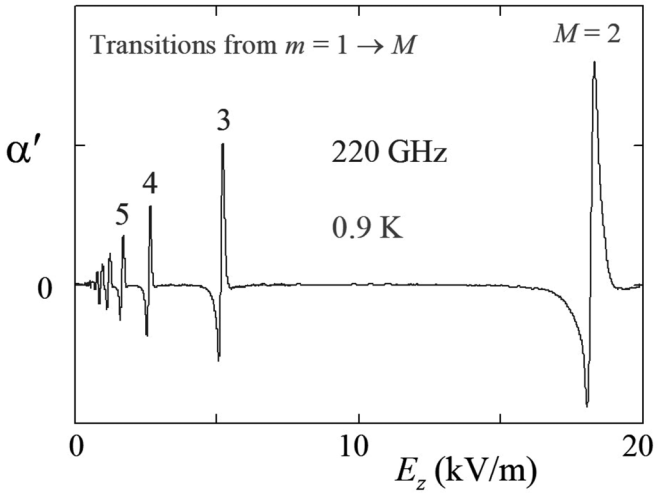

FIG. 2. Differential microwave absorption α' at 220 GHz as the vertical holding field E_z was swept, showing resonant transitions from the ground state (subband), $m = 1$, to higher Rydberg states (subbands) $m = M$ (with M up to 12 observed).

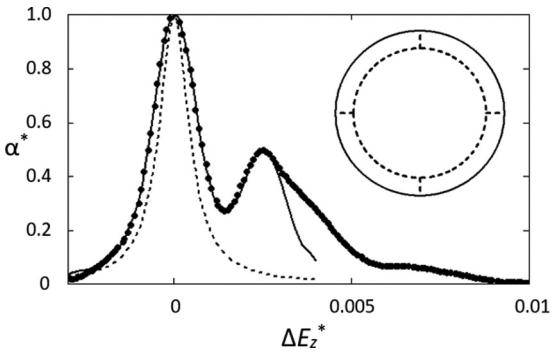

FIG. 3. Measured absorption line shape α at 189.6 GHz at 0.304 K, normalized to the first maximum and plotted against the fractional change in vertical electric field as the voltage is swept. The inset shows the electrode geometry [23], outer radius 28 mm, with the four ring segments in the lower electrode, inner radius 22 mm. The solid line shows a Lorentzian, $\gamma = 5.04 \times 10^{-4}$ (dashed line), broadened by a field modulation of 10 mV rms. The second peak has a relative magnitude 0.46 and a field offset $\delta = -0.0028$.

from the ground state to the first excited state, $M = 2$ [2,6]. The f_{21} resonance was measured over the frequency range 165 to 220 GHz at 1.2 K [2], corresponding to an electric field range $6 < E_z < 18\,\mathrm{kV/m}$. Most measurements were made at a fixed microwave frequency of 189.6 GHz at $E_z \approx 10.6\,\mathrm{kV/m}$ where a local maximum in the cell response was observed. The field E_z was tuned through resonance for a range of electron densities and temperatures. The incremental increase in the resonant frequency f_{21} at 189.6 GHz corresponds to 2.44 GHz/volt for a sweep in the pressing field voltage V_z.

B. Absorption line shape

The measured differential absorption α' was integrated numerically to give the absorption line shape $\alpha(V_z, T)$. Above 1 K it is close to a Lorentzian, but at low temperatures and low microwave power it can have a complex structure as shown in Fig. 3 at 0.304 K and in Fig. 4 at 0.304, 0.855, and 1.004 K. The data in Fig. 4 are plotted against the pressing voltage V_z while in Fig. 3 they are plotted against the fractional change ΔE^* in the vertical electric field E_z. as V_z is swept through the resonance ($\Delta E^* = 0$). Two resonance peaks are seen very close together which reflect the electrode geometry.

Both peaks at 0.304 K can be precisely fitted by a Lorentzian, linewidth (dotted line) $\gamma = 27 \pm 2\,\mathrm{MHz} \equiv 11\,\mathrm{mV} = 5.04 \times 10^{-4}$ in the fractional field, broadened by the small ac modulation of 10-mV rms (6.4×10^{-4} in the fractional field). The offset second peak with the same parameters is followed by a long tail.

Sloggett *et al.* [26] numerically analyzed the vertical electric field distribution in circular disk capacitors, defining δ as the fractional change in field compared to infinite electrodes with the same spacing and voltage. The field is maximum at the center with a deviation $\delta_0 = -2.57\ \exp(-6.079\,R/D)$.

It decreases exponentially towards the edges as $\delta(r) = -\exp[-(1 + 2\pi(R - r)/D)]$, reaching $\delta \approx -0.01$ at 1 mm from the outer edge of the capacitor. The first peak comes from electrons between the 22-mm radius central electrodes ($\delta_0 \approx -2.3 \times 10^{-29}$) with 59% of the electrons. There is a 0.5-mm

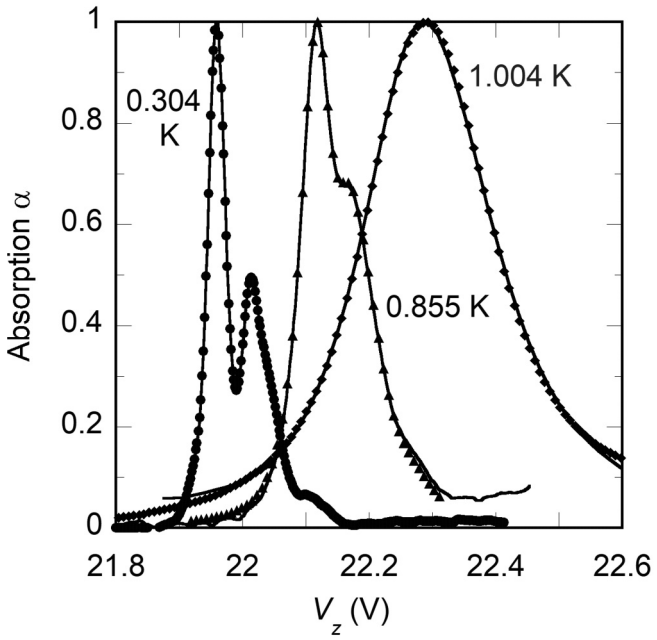

FIG. 4. Temperature-dependent line shapes. The inhomogeneously broadened line shape is shown at 0.304 K (●). The line shape broadens as the temperature increases as shown at 0.855 K (■) and 1.004 K (♦). The lines through the points show the convolution of the 0.304-K line shape with a Lorentzian line shape with $\gamma = 49\,\mathrm{MHz}$ at 0.855 K and 288 MHz at 1.004 K. The line shapes have been normalized to their peak values. The position of the line is temperature dependent, as discussed in the text.

gap between the central and ring electrodes. This gives a small decrease in E_z over the gap region. The second peak comes from electrons (26% of the total) between the ring electrodes with a central fractional field offset of $\delta_0 = -0.0028$, in good agreement with Sloggett for an electrode size of 4.5 mm. The tail comes from the remaining 15% of electrons under the gap and around the edge where the field reaches $\delta \approx -0.01$ at the edge of the electron sheet, as seen in Fig. 3. The rms inhomogeneity in E_z across the electron sheet is 0.2%.

However, the linewidth of 27 MHz at 0.3 K can only be regarded as an upper limit for any residual or zero-point linewidth. A rms variation of only 1 μm in the electrode separation across the 56-mm diameter would give a residual linewidth of some 38 MHz (7×10^{-4} in the fractional field). Other small effects on the line shape at this level could include nonparallelism of the electrode plates, a tilt in the helium surface, and standing waves in the microwave intensity.

We used the experimental line shape at $T_0 = 0.3\,\mathrm{K}$ as a reference $\alpha_0(V_z)$ for analysis at higher temperatures, convolving it with a temperature-dependent Lorentzian to obtain $\gamma(T)$. The precision (<1 MHz) of these fits was excellent (solid lines in Fig. 4), clearly showing both peaks broadening and shifting together.

In the low-power limit, the area of the line should be proportional to the total number of electrons and the incident microwave power. Experimentally, the area was indeed independent of T at low powers. The area was used to estimate the electron density for each set of data, relative to reference data sets in which the density was measured directly from

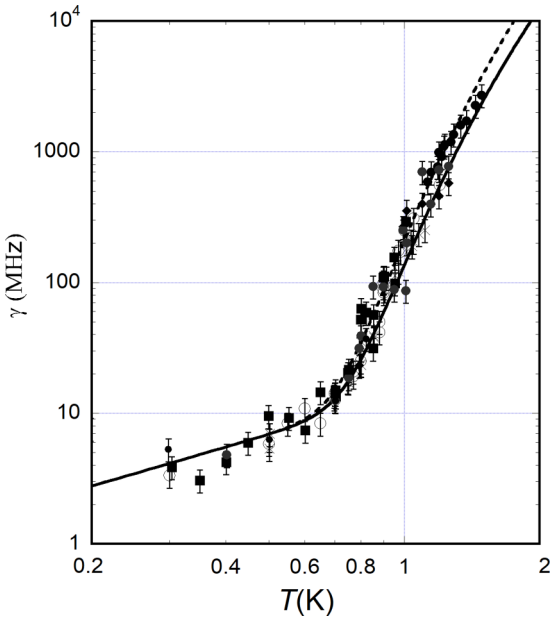

FIG. 5. Temperature-dependent contribution to the Lorentzian linewidth $\gamma(T)$ versus temperature at 189.6 GHz. Measurements of the line-shape height and width (■, ●) were used to obtain $\Delta\gamma(T) = \gamma(T) - \gamma(0.3)$, relative to the value at 0.3 K. Data from Grimes *et al.* [2], scaled for the different pressing field, are shown (○). The solid line is the theory by Ando [13], while the dashed line shows Ando's theory with the vapor-atom scattering contribution scaled by a factor of 1.6.

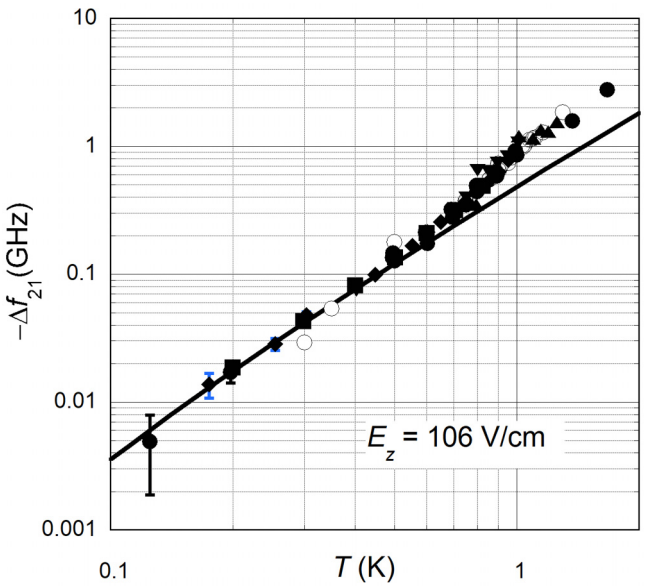

FIG. 6. Temperature-dependent resonance shift $\Delta f_{21}(T) = f_{21}(T) - f_{21}(0)$ at 189.6 GHz. The resonance position moved to higher values of V_z at higher temperatures. The voltage shift was converted to a frequency shift using the factor 2.44 GHz/V. The electron densities were 0.67 (▲), 1.0 (▼), 1.5 (♦), 1.7 (○), and 2.4 (■)$\times 10^{11}$ m^{-2}. Other data points (●) were for various electron densities. The solid line shows the theoretical calculations of Dykman *et al.* [22] due to ripplon renormalization.

the magnetoconductivity. The typical electron density for the linewidth data presented here was 1.7×10^{11} m^{-2}, although densities up to 6.5×10^{11} m^{-2} were used. No dependence of the linewidth on the electron density was observed. At higher powers and temperatures above about 1.5 K, we gradually started to lose electrons.

At higher microwave powers, we observed power broadening, absorption saturation, nonlinear effects, and hysteresis. The Lorentzian linewidth becomes power dependent: $\gamma_P^2 = \gamma^2 + \gamma\tau\Omega^2 = \gamma^2 + bP$, where the incident microwave power $P \propto E_{\rm RF}^2 \propto \Omega^2$, where $\Omega = eE_{\rm RF}z_{12}/\hbar$ is the Rabi frequency, $E_{\rm RF}$ is the microwave field amplitude, and $1/\tau$ is the spontaneous decay rate from the excited state. This leads to absorption saturation and power broadening. At low powers, we recover a Lorentzian line shape, Eq. (4).

C. Temperature-dependent linewidth

The line shape was analyzed to obtain $\Delta\gamma(T) = \gamma(T) - \gamma(0.3)$. From Eq. (7) the theoretical temperature-dependent linewidth $\gamma(T) = AT + CN_g(T)/N_g(1)$, where the first term is due to ripplon scattering and the second to vapor atom scattering. The experimental reference value of $\gamma(0.3)$ was determined by a linear fit of the temperature dependence of $\Delta\gamma(T)$ below 0.7 K and extrapolating to zero temperature, following Eq. (7). The resultant experimental values of $\gamma(T)$ are shown in Fig. 5. The solid line shows numerical calculations of $\gamma(T)$ from Ando's theory [13], with $A = 12.8$ MHz/K and $C = 109$ MHz. The transition from gas-atom to ripplon scattering is clearly seen at about 0.7 K. The fit below 0.7 K is good, although with only a few data points. The dashed line shows the vapor-atom scattering scaled up by a factor of 1.6 in agreement with Isshiki *et al.* [7].

D. Temperature-dependent resonant frequency

We also found that the resonant frequency itself was unexpectedly, and rather strongly, temperature dependent. The experiments were done at a fixed microwave frequency of 189.6 GHz for a range of electron densities n. The resonant absorption frequency of the electrons was tuned using the Stark effect by sweeping the top-plate voltage V_z and hence the vertical electric field E_z.

Following the line-shape analysis, the voltage $V_{21}(T)$ at resonance was obtained from 0.1 to 1.5 K, for a range of electron densities n. As the temperature increased, the voltage increased as shown in Fig. 4. This corresponds to a decrease in the resonant frequency $f_{21}(T)$ as the temperature increases, with a scaling factor of 2.44 GHz/volt.

To convert this to a frequency shift from zero temperature, $\Delta f_{21}(T) = f_{21}(T) - f_{21}(0)$, we require a zero-temperature reference voltage $V_{21}(0)$ which would be the resonant position at $T = 0$. For each of the two long experimental runs the data were extrapolated to zero temperature by fitting to a power law $\Delta f_{21}(T) = -AT^\alpha$. An excellent fit over the whole temperature range was found with $A = 810 \pm 100$ MHz and $\alpha = 2.5 \pm 0.2$. In practice the reference voltage was very constrained, leading to an uncertainty of less than ± 3 MHz at 0.1 K, which is very small compared to 189.6 GHz and to the 810-MHz shift at 1 K. The resonant frequency decreased by 0.43% at 1 K. The data are plotted in Fig. 6.

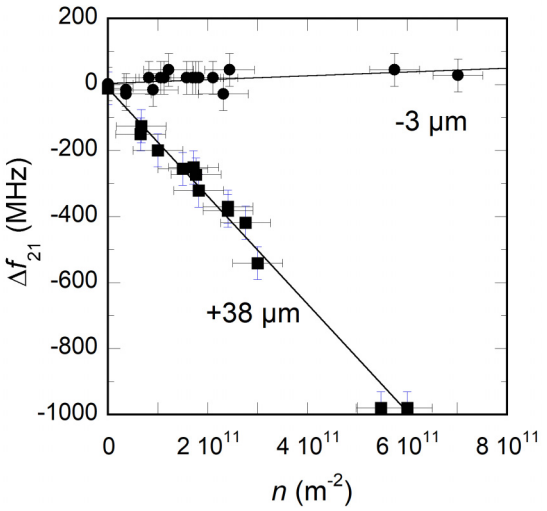

FIG. 7. Change in resonant frequency, extrapolated to zero temperature, versus the electron density n for two separate experimental runs. The lines show the predicted density dependence if the helium level lies 3 μm below (●), and 38 μm above (■) the center of the cell capacitor, respectively.

The measured shift $\Delta f_{21}(T)$ is independent of electron density as shown for experimental runs with electron densities from 0.67 to 2.4×10^{11} m^{-2}. Some spot points were also taken at densities up to 6.5×10^{11} m^{-2}. It is also independent of the microwave power in the low-power limit and of the liquid-helium level in the cell (but see Sec. III E below).

The resonant frequency shift $\Delta f_{21}(T)$ is due to ripplons on the helium surface but the theory is subtle, challenging, and interesting as shown recently by Dykman *et al.* [22]. The electron energy spectrum is renormalized by interactions with zero-point and thermal ripplons. In particular, two-ripplon processes result in nonzero diagonal matrix elements of the interaction Hamiltonian and are responsible for temperature-dependent Lamb-like shifts of the eigenvalue energies. The final result for the theoretical temperature-dependent frequency shift $\Delta f_{21}(T)$ for $E_z = 106$ V/cm is plotted in Fig. 6. Given that there are no adjustable parameters in the calculations, this agreement is good, particularly below 1 K.

E. Density-dependent resonant frequency

The temperature-dependent frequency shift was independent of the electron density. But, for a given pressing voltage V_z, the electric field E_z and hence the resonant frequency will depend on the electron density through Eq. (8c), if the helium level is not precisely at the center of the capacitor plates [2], giving a voltage offset and an apparent density-dependent frequency shift. In the two runs where this was investigated, the resonance position in V_z and the equivalent frequency shift Δf_{21} varied linearly with the electron density n, as shown in Fig. 7. This corresponds to the liquid-helium surface being 38 μm above and 3 μm below the center of the cell for the two runs, respectively. This gives an additional electric field E_z proportional to n, from the second term in Eq. (8c). The measured temperature-dependent frequency shifts were the same in both cases, within the error bars.

This enables us to eliminate another possible cause of a resonant frequency shift with temperature, from changes in the helium level. The surface tension η decreases with temperature and could change the helium level, through capillary rise, although the change in η is small, 2% at 1 K [27]. The level will also fall due to an increasing helium vapor density above 1 K. This would give a temperature-dependent field E_z, through Eq. (8c), and a temperature-dependent frequency shift. But, this would be density dependent, particularly at higher temperatures, which was not observed. Using Eq. (8), we estimate that the frequency shift for a height change would be 1.5 MHz/μm for no electrons; -2.8 MHz/μm for $n = 1\times10^{11}$ m^{-2}; and -8.8 MHz/μm for $n = 2.4\times10^{11}$ m^{-2}. We conclude that any changes in the helium height did not contribute to the temperature-dependent frequency shifts, within the error bars. The Corbino current measurements confirmed that the change in helium level was less than 2 μm below 1.4 K.

Some measurements were made in the Wigner crystal, below the melting temperature $T_m = 0.225\times10^{-6}\, n^{1/2}$ K [28]. For the highest density used here $n = 6.7\times10^{11}$ m^{-2}, $T_m = 0.181$ K. No effects were observed but no systematic measurements were made.

IV. CONCLUSION

We have presented measurements of the resonant microwave absorption by the Rydberg energy levels of surface-state electrons on superfluid helium, in the frequency range 165–220 GHz [6,23]. The differential absorption was measured and integrated to give the microwave absorption line shape. Direct measurements of the absorption line were made using large-amplitude square-wave modulation.

The microwave line shape was measured at low microwave powers from 0.1 to 1.5 K. The small temperature-independent residual line shape at low temperatures may be due to inhomogeneous broadening. A convolution analysis was used to determine the temperature-dependent Lorentzian contribution to the linewidth $\gamma(T)$ for excitation to the first excited state. In the ripplon-scattering region below 0.7 K, the experimental results are consistent with the theory by Ando [13]. In the gas atom-scattering regime, the linewidth is proportional to the vapor atom number density, as expected, but with a scaling factor of 1.6 above Ando's numerical result, confirming a previous analysis by Isshiki *et al.* [7].

The resonant frequency was found to be temperature dependent, decreasing as temperature increases. Below 1 K this is in good agreement with a recent theory by Dykman *et al.* [22] based on the renormalization of the electron energy spectrum due to dynamic interactions with ripplon excitations, analogous to a Lamb shift in the electronic energy levels.

ACKNOWLEDGMENTS

We thank A. J. Dahm, J. Goodkind, K. Kono, S. A. Lyon, P. J. Meeson, Y. Mukharsky, P. M. Platzman, J. Saunders, and especially M. I. Dykman and D. Konstantinov for discussions and F. Greenough, A. K. Betts, and others for technical support. The work was supported by the EPSRC (UK) Grant No. GR/R12602, by the EU Human Potential Programme under Contract No. HPRN-CT-2000-00157 *Surface Electrons*, and by Royal Holloway, University of London.

[1] *Two Dimensional Electron Systems on Helium and Other Cryogenic Substrates*, edited by E. Y. Andrei (Kluwer, New York, 1997); Y. P. Monarkha and K. Kono, *Two-Dimensional Coulomb Liquids and Solids* (Springer-Verlag, Berlin, 2004).

[2] C. C. Grimes, T. R. Brown, M. L. Burns, and C. L. Zipfel, Phys. Rev. B **13**, 140 (1976); C. L Zipfel, T. R. Brown, and C. C. Grimes, Phys. Rev. Lett. **37**, 1760 (1976); C. C. Grimes and T. R. Brown, *ibid.* **32**, 280 (1974).

[3] D. K. Lambert and P. L. Richards, Phys. Rev. Lett. **44**, 1427 (1980); Phys. Rev. B **23**, 3282 (1981).

[4] V. S. Édel'man, Zh. Eksp. Teor. Fiz. **77**, 673 (1979) [Sov. Phys. JETP **50**, 338 (1979)].

[5] A. P. Volodin and V. S. Édel'man, Zh. Eksp. Teor. Fiz. **81**, 368 (1981) [Sov. Phys. JETP **54**, 198 (1981)].

[6] E. Collin, W. Bailey, P. Fozooni, P. G. Frayne, P. Glasson, K. Harrabi, M. J. Lea, and G. Papageorgiou, Phys. Rev. Lett. **89**, 245301 (2002).

[7] H. Isshiki, D. Konstantinov, H. Akimoto, K. Shirahama, and K. Kono, J. Phys. Soc. Jpn. **76**, 094704 (2007).

[8] D. Konstantinov, M. I. Dykman, M. J. Lea, Y. Monarkha, and K. Kono, Phys. Rev. Lett. **103**, 096801 (2009).

[9] D. Konstantinov, H. Isshiki, Y. Monarkha, H. Akimoto, K. Shirahama, and K. Kono, Phys. Rev. Lett. **98**, 235302 (2007); D. Konstantinov, M. I. Dykman, M. J. Lea, Yu. P. Monarkha, and K. Kono, Phys. Rev. B **85**, 155416 (2012); A. D. Chepelianskii, M. Watanabe, K. Nasyedkin, K. Kono, and D. Konstantinov, Nat. Commun. **6**, 8210 (2015).

[10] D. Konstantinov and K. Kono, Phys. Rev. Lett. **105**, 226801 (2010).

[11] D. Konstantinov, A. Chapelianski, and K. Kono, J. Phys. Soc. Jpn., **81**, 093601 (2012).

[12] D. Konstantinov, Yu. Monarkha, and K. Kono, Phys. Rev. Lett. **111**, 266802 (2013).

[13] T. Ando, J. Phys. Soc Jpn., **44**, 765 (1978).

[14] M. M. Nieto, Phys. Rev. A **61**, 034901 (2000).

[15] F. Stern, Phys. Rev. B **17**, 5009 (1978).

[16] M. V. Rama Krishna and K. B. Whaley, Phys. Rev. B **38**, 11839 (1988).

[17] E. Cheng, M. W. Cole, and M. H. Cohen, Phys. Rev. B **50**, 1136 (1994).

[18] M. H. Degani, G. A. Farias, and F. M. Peeters, Phys. Rev. B **72**, 125408 (2005).

[19] M. W. Cole, Phys. Rev. A **1**, 1838 (1970).

[20] L. B. Lurio, T. A. Rabedeau, P. S. Pershan, I. F. Silvera, M. Deutsch, S. D. Kosowsky, and B. M. Ocko, Phys. Rev. Lett. **68**, 2628 (1992); **72**, 309(E) (1994); Phys. Rev. B **48**, 9644 (1993).

[21] K. Penanen, M. Fukuto, R. K. Heilmann, I. F. Silvera, and P. S. Pershan, Phys. Rev. B **62**, 9621 (2000).

[22] M. I. Dykman, D. Konstantinov, K. Kono, and M. J. Lea [Phys. Rev. Lett. (to be published)], arXiv:1707.02946.

[23] See Supplemental Material at http://link.aps.org/supplemental/10.1103/PhysRevB.96.235427 for details of the microwave system and experimental cell.

[24] P. V. E. McClintock, University of Lancaster (private communication).

[25] M. J. Lea, P. Fozooni, A. Kristensen, P. J. Richardson, K. Djerfi, M. I. Dykman, C. Fang-Yen, and A. Blackburn, Phys. Rev. B **55**, 16280 (1997).

[26] G. J.Sloggett, N. J. Barton, and S. J. Spencer, J. Phys. A: Math. Gen. **19**, 2725 (1986).

[27] K. R. Atkins, Can. J. Phys. **31**, 1165 (1953); K. R. Atkins and Y. Narahara, Phys. Rev. **138**, A437 (1965).

[28] G. Deville, J. Low Temp. Phys. **72**, 135 (1988).